Supplementary Information

1. Experimental

1.1 Sample preparation

1.1.1 Materials

Zirconium tetrachloride ($ZrCl_4$, 99.9%), formic acid (HCOOH, 99%), poly (4-styrene sulfonic acid) (PSS) and 2-amino terephthalic acid (H_2ATA, 99%) were purchased from Aladdin Industrial Corporation, polyether amine of M2070 (M2070) were achieved from Shanghai Macklin Biochemical Co., Ltd, N, N-dimethylformamide (DMF, 99.5%), acetone (CH_3COCH_3, 99%), ethanol (C_2H_5OH, 99.7%) and triethanolamine (TEOA, 99.5%) were obtained from Sinopharm Chemical Reagent Co., Ltd. Deionized water was used throughout all experiments. $^{12}CO_2$ was of 99.999% purity and was obtained from Zhenjiang Zhongpu Special Gas Co., Ltd. $^{13}CO_2$ of 99% purity was obtained from Guangzhou Xizhou Gas Co., Ltd. All chemicals were of analytical grade and were used without further purification.

1.1.2 Syntheses of NH_2-UIO-66

NH_2-UIO-66 was synthesized according to the reported method, and some modifications were made. The detailed preparation steps for synthesis were: First, $ZrCl_4$ (0.233 g, 1 mmol) and H_2ATA (0.181 g, 1 mmol) were dissolved in DMF (100 mL). After half an hour of ultrasound and then the obtained mixed solution was transferred to a 100 mL polytetrafluoroethylene autoclave, followed by heating at 120°C for 12 h to obtain crystals. The resulting white microcrystalline powders were cooled to room temperature, centrifuged and washed with high-speed centrifuge (washed three times with DMF, acetone and ethanol respectively). Finally, the obtained product was dried in an oven at 150℃ for 12 h.

1.1.3 Syntheses of NH_2-UIO-66-LV

As shown in Scheme 1a, firstly, $ZrCl_4$ (0.233 g, 1 mmol) and H_2ATA (0.181 g, 1 mmol) were dissolved in DMF (100 mL). After that, 4.3 mL of HCOOH was added as modulators. After half an hour of ultrasound and then the obtained mixed solution was

transferred to a 100 mL polytetrafluoroethylene autoclave, followed by heating at 120°C for 12 h to obtain crystals. The resulting white microcrystalline powders were cooled to room temperature, centrifuged and washed with high-speed centrifuge (washed three times with DMF, acetone and ethanol respectively). Subsequently, the obtained product was dried in an oven at 150℃ for 12 h. Finally, the dried product was placed in a tube furnace and calcined at 250℃ in N_2 atmosphere for 2 h to obtain the final product NH_2-UIO-66-LV.

1.1.4 Syntheses of [M2070][PSS] porous ionic liquids ([M2070][PSS] PIL)

As shown in Scheme 1b, firstly, 18.7 mL of polyether amine M2070 was added to 5.5 mL of PSS solution. Then add an appropriate amount of deionized water and sonicate the mixed solution for 2 h to fully dissolve it. Finally, evaporate the water through an 80℃ oil bath until the volume of the mixture no longer decreased, and then stop evaporation. The resulting solution was [M2070][PSS] PIL.

1.1.5 Synthesis of heterojunction type porous liquids photocatalyst (NH_2-UIO-66-LV PL)

As shown in Scheme 1c, firstly, 0.2 g of NH_2-UIO-66-LV and 1.2 g of [M2070][PSS] PIL were dissolved in 20 mL of deionized water and subjected to ultrasound treatment for 10 minutes. Then, the NH_2-UIO-66-LV suspension was added to the [M2070][PSS] PIL solution, and the resulting mixed solution was vigorously stirred at room temperature for half an hour to fully dissolve. Finally, the solvent was evaporated through an oil bath at 65℃ until it reached 1/10 of the mixed solution, and the evaporation was stopped. The resulting solution was dried in a vacuum drying oven at 65℃ for 24 h to obtain NH_2-UIO-66-LV PL, which is a heterojunction type UIO-66 based porous liquid photocatalyst.

1.2 Photocatalytic CO_2 Reduction Measurements

10 mg of photocatalyst was mixed in a 20-ml solution containing 18 ml of deionized water and 2 ml of TEOA in a 100 ml quartz glass reactor. After that, the reaction setup was purged by pure CO_2 gas (purity >99.999%) for 10 min and then vacuum-pressure-treatment more than twice to ensure all the impurities and trapped air

were completely removed. Before illumination, the reactor was installed to CEL-SPH2N system (Beijing China Education Au-light Co., Ltd) equipped with a 300 W Xe lamp which was used to simulate sunlight. Then turn on the xenon lamp, take the gas every 1 hour, and turn off the xenon lamp after 5 h of light reaction to retain the mixed solution after the reaction. Gas chromatography (GC-2030) was applied to analyzed the possible gaseous and liquid products by the detectors of a thermal conductivity detector and a flame ionization detector. The carrier gas was Ar with a flow rate of 20 mL/min and the column temperature was 333 K.

1.3 Characterizations

The crystal structure of the sample was detected by X-ray diffraction (XRD) patterns, which were detected by a D/max-RA X-ray diffractometer (Rigaku, Japan) and Ni-filtrated Cu Ka radiation (40 kV, 200 mA). The functional group structure of the sample was characterized by Fourier transform infrared spectroscopy (FT-IR), which were detected on a Nicolet Nexus 470 FT-IR (America thermo-electricity Company). Thermogravimetric analysis (TGA) was obtained on a TGA Q50 TA instrument under N_2 atmosphere (heating rate of 10 °C/min, temperature range of 25 ~ 700 °C). The elemental analysis of the prepared sample was obtained by X-ray photoelectron spectroscopy (XPS) (Shimadzu Co., Japan), which were detected by a Kratos Axis-Ultra DLD spectrometer with a monochromatized Al Kα line source (150 W), using anode monochromatic AI target. The morphology and structure of synthesized samples were analyzed by scanning electron microscopy (SEM, JSM-7800F, Japan) with the energy dispersive spectroscopy analysis (EDS) attached part, transmission electron microscopy (TEM, JEM-2100, 200 kV, Japan). Nitrogen adsorption and desorption experiments were measured by Tristar II 3020 M. During the measurement, the prepared samples were dried in a vacuum at 120℃ for 6 h. The specific surface area and the corresponding pore size distribution were obtained by Bruner-Emmett-Taylor (BET) and Barrett-Joyner-Harunda (BJH) methods, respectively. Differential scanning calorimetry (DSC) curves were measured through the DSC Q 100 TA instrument under N_2 atmosphere at a heating rate of 10 ℃ /min. The light absorption range of the prepared sample was detected by UV–vis diffuse

reflectance spectra (UV–vis DRS), which were detected by a 2450 spectrometer (Shimadzu Co., Japan) equipped with an integrated sphere accessory for diffused reflectance spectra, using $BaSO_4$ as a reference. The fluorescence intensity of samples was characterized by photoluminescence (PL) spectra, which was measured with a Cary Eclipse Spectrophotometer at an excitation wavelength of 350 nm. In situ diffuse reflectance infrared Fouier transform spectroscopy (DRIFTS) were acquired from Thermo Scientific Nicolet iS50. The gas products were analyzed using a gas chromatograph (GC-2030) equipped with a flame ionized detector and thermal conductivity detector. The ^{13}C mass spectra were recorded on a Shimadzu GCMS-QP2020 system.

1.4 Photoelectrochemical measurements

The electrochemical measurement (CHI-760E, Shanghai Chenhua Instrument Co., Ltd, China) was performed in a conventional three-electrode cell on a typical electrochemical workstation. In the photocurrent measurement, a Pt wire electrode was used as the counter electrode and a saturated calomel electrode (SCE) acted as the reference electrode. The working electrodes were prepared by using the as-prepared samples covered on the surface with Indium tin oxide (ITO) conductor glass, and the effective working area is 1 * 1 cm^2. The quartz cell measurement system was filled with 1 M Na_2SO_4 (pH = 7.0) electrolyte for the photocurrent testing (Bias voltage: 0 V; lighting time interval: 30 s (light on for 30 s, turn off for 30 s)), and the Mott-Schottky curves measurement (experiment was performed in dark: frequency was 1000 Hz; amplitude was 5 mV; potential range was from -1 V to 1 V with step width 0.05 V.). While the electrochemical impedance spectroscopy (EIS) was tested in the 5 mM potassium ferricyanide, and 0.1 M KCl mixture (EIS test frequency range from 0.1 Hz to 100K Hz).

1.5 Cycle experiment

In each run, the condition was fixed (irradiation time, 5 h; sampling, 3 times). After one run, 10 mL acetonitrile and 2 mL TEOA were replenished into the reaction system, followed by CO_2 aeration and light irradiation. Other steps were consistent with photocatalytic CO_2 reduction. After 3 cycles, the sample was recovered by

centrifugation and drying.

1.6 CO_2 adsorption experiment

The CO_2 adsorption tests were conducted within the homemade reactor. Generally, weighed about 0.1 g of sample into a small beaker and placed it in the center of the reactor. After that the sample was degassed in vacuum at 25℃ for 0.5 h, the pure CO_2 (99.999%) with certain flow was led to the reactor for 5 min to reach a solubility equilibrium. After that, closed the outlet valve and adjusted the pressure to 0 bar, continue to place for 5 min. Subsequently the small beaker was taken out and weighed by analytical balance. Thereafter, repeated the above steps, adjusted the pressure to 1, 2, 3, 4 bar respectively and weighed.

1.7 EPR Measurements

Electron paramagnetic resonance (EPR) measurements were implemented at a SPINSCAN X-benchtop EPR spectrometer; a new EPR unit from ADANI, Belarus, operated at the CW X-band, internal frequency counter, and was fully auto-tuned. The spectrometer ran at a modulation frequency and amplitude of 100 kHz and 0.1 G, respectively. Its microwave frequencies cross checked with a Hewlett-Packard 5342 A microwave frequency counter. In typical measurements, each sample (25 mg) was suspended in a solvent mixture formed from: a 0.2 mL mixture of triethanolamine and water (1:10 v/v, respectively). The solution was then placed in a capillary glass tube, which was then sealed and positioned at the active zone of the rectangular resonator of the EPR-spectrometer. All the investigated samples were measured at room temperature (300 K) in the dark and after irradiation with a white light source simulating sunlight.

2 Figures and tables

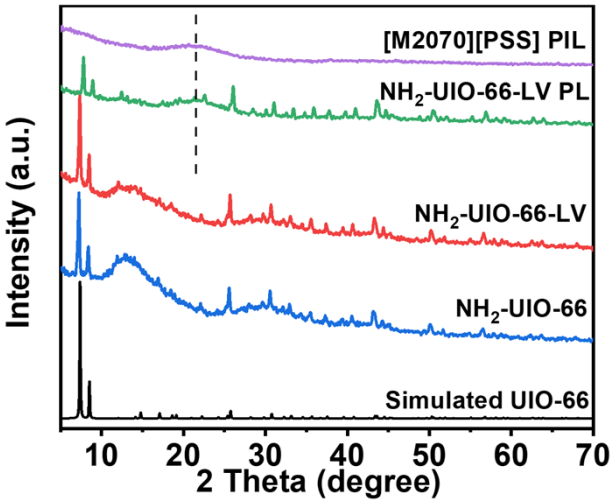

Figure.S1 XRD patterns of different samples.

As shown in Figure S1, the diffraction peaks of NH_2-UIO-66-LV and NH2-UIO-66 were basically consistent, and could match the diffraction peaks of the fitted UIO-66, indicated that introducing defects in NH_2-UIO-66 did not affect its original crystal structure. In addition, [M2070][PSS] PIL only exhibited a wide and strong diffraction peak at $2\theta=21.5^\circ$, indicated its amorphous structure. In contrast, NH_2-UIO-66-LV PL also exhibited a wide diffraction peak at around $2\theta=21.5^\circ$, while maintaining other diffraction peaks at the same position as NH_2-UIO-66-LV, indirectly proved the successful synthesis of NH_2-UIO-66-LV PL.

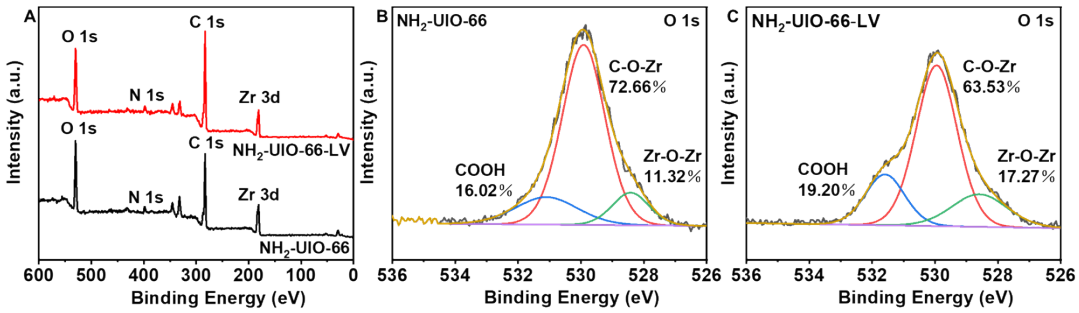

Figure.S2 XPS spectra (D, E and F) of different samples.

As shown in Figure S2A, both NH_2-UIO-66 and NH_2-UIO-66-LV had peaks corresponded to O 1s, N 1s, C 1s and Zr 3d, demonstrated the structural integrity. In addition, as shown in Figures 2B and 2C, the content of C-O-Zr bonds in the O 1s high-resolution XPS spectrum of NH_2-UIO-66-LV was significantly reduced compared to NH_2-UIO-66, indicated the absence of organic ligands, thereby proved the successful formation of defects in NH_2-UIO-66-LV.

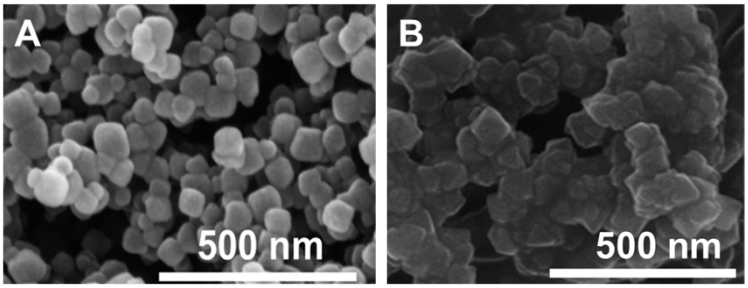

Figure.S3 SEM images of NH_2-UIO-66-LV (A) and NH_2-UIO-66 (B)

As shown in Figure S3A and S3B, both samples were octahedral in shape with a size of about 100nm. However, compared to NH_2-UIO-66, the defective NH_2-UIO-66-LV sample had significantly higher crystallinity and more regular particle shape, which also proved that the introduction of defects could regulate the morphology of NH_2-UIO-66, which may be more conducive to photocatalytic reactions.

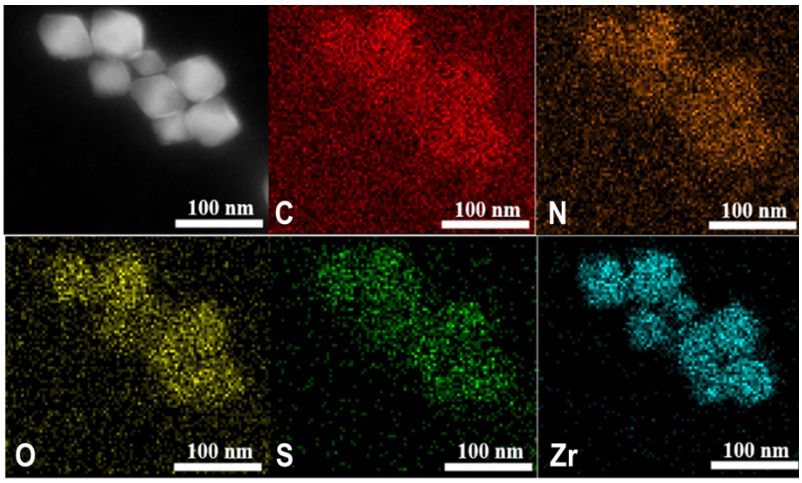

Figure.S4 TEM images and EDS mapping of NH_2-UIO-66-LV PL

and isotope experiment in photocatalytic CO_2 reduction of NH_2-UIO-66-LV PL

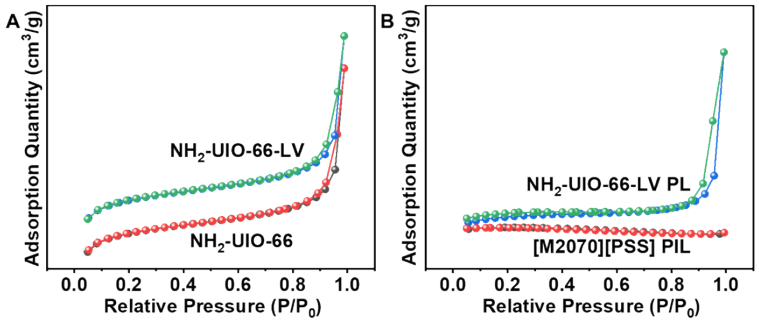

Figure.S5 N_2 adsorption-desorption isotherms of different samples (A and B)

N_2 adsorption desorption experiments were conducted to analyze the specific surface area and pore volume of the two MOFs. As illustrated in Figure S5A, the adsorption isotherm of NH_2-UIO-66-LV was identified as a typical Type I isotherm, which confirmed the presence of micropores as described in the literature, but these pores were demonstrated to be excessively small for [M2070][PSS] PIL. In addition, as shown in Table 1(Supporting Materials), the specific surface area and pore volume of NH_2-UIO-66-LV were 1029.07 m^2 g^{-1} and 0.17 cm^3 g^{-1}, respectively, which were significantly higher than those of NH_2-UIO-66 (665.82 m^2 g^{-1} and 0.09 cm^3 g^{-1}), indicated the successful formation of defects in NH_2-UIO-66-LV. As shown in Figure S5B, due to the low solubility of N_2 molecules in NH_2-UIO-66-LV PL and [M2070][PSS] PIL, the N_2 adsorption capacity of both samples was lower than the detection limit of the specific surface area and porosity analyzer. However, it was worth noting that due to the retention of good permanent porosity in NH_2-UIO-66-LV PL, the N_2 adsorption capacity has been slightly improved compared to [M2070][PSS] PIL.

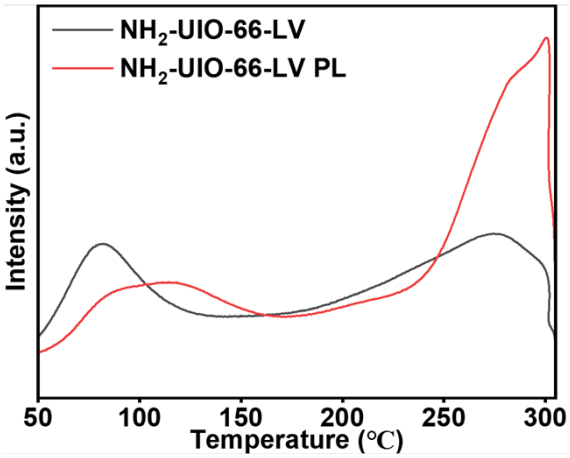

Fig.S6 CO_2-TPD of NH_2-UIO-66-LV and NH_2-UIO-66-LV PL.

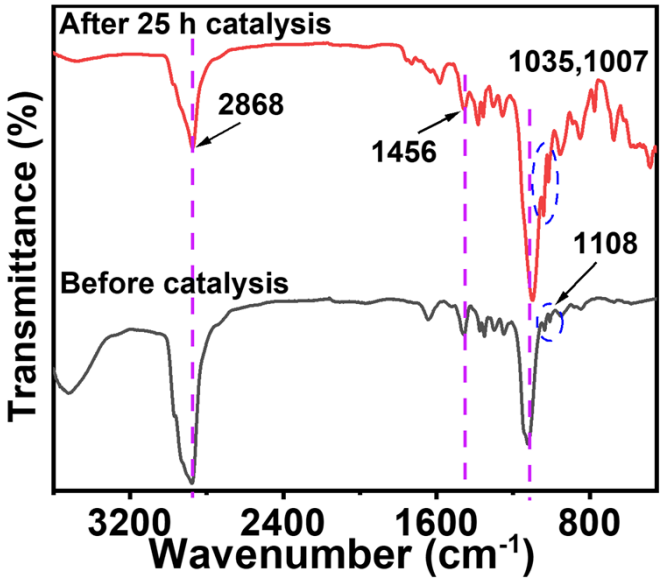

Figure.S7 FT-IR spectra of NH_2-UIO-66-LV PL before and after 25 h photocatalytic reaction

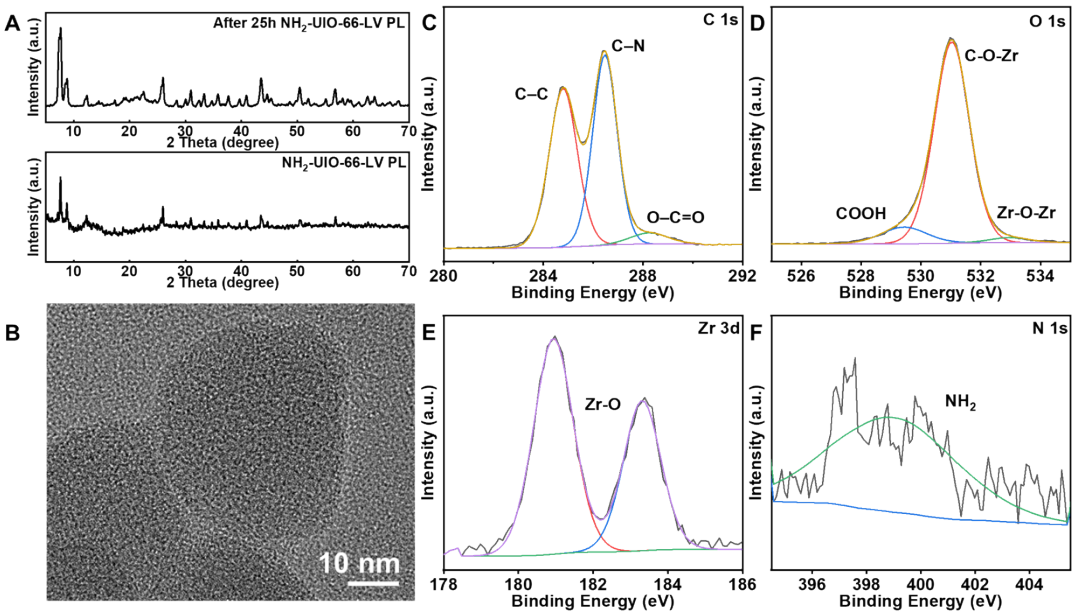

Figure.S8 XRD patterns of different samples(A), TEM image of NH_2-UIO-66-LV PL after reacted 25h (B) and XPS spectra (C, D, E and F) of NH_2-UIO-66-LV PL after reacted 25h

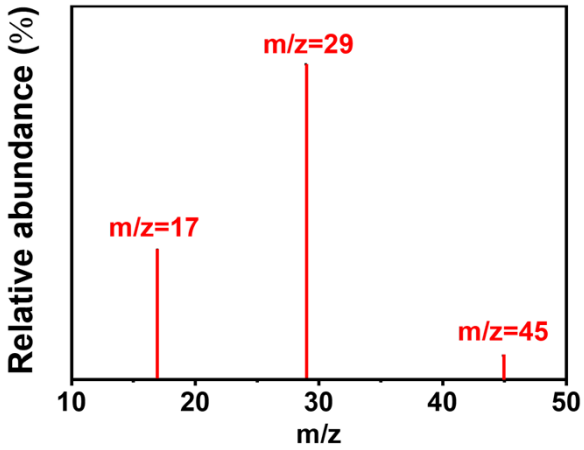

Figure.S9 isotope experiment in photocatalytic CO_2 reduction of NH_2-UIO-66-LV PL

To determine the carbon source of the CO_2 photoreduction products, an isotope tracing experiment was designed and conducted using $^{13}CO_2$ instead of the original CO_2 as the carbon source (as illustrated in Figure S9). The generated gases were analyzed via gas chromatography-mass spectrometry (GC-MS), and the detected peaks with mass-to-charge ratios (m/z) of 17, 29, and 45 were identified as $^{13}CH_4$, ^{13}CO, and $^{13}CO_2$, respectively. This result confirmed that the generated products were indeed derived from CO_2.

Table S1 Specific surface area and total pore volume of different samples

Samples	Specific surface area (m^2/g)	Pore volume (cm^3/g)
NH_2-UIO-66	665.82	0.09
NH_2-UIO-66-LV	1,029.07	0.17
NH_2-UIO-66-LV PL	3.65	0.003
[M2070][PSS] PIL	-2.13	-0.000079

Table S2 Comparison of CO_2 photoreduction performance of UIO-66-based photocatalysts.

Sample	Condition	Reduction rate (μmol g^{-1} h^{-1})
TiO_2/UIO-66/Cu[1]	Visible light H_2O	CO: 21.69 CH_4: 2.27
UIO-66/CuS[2]	300 W Xe-lamp 1.5 mL H_2O	CO: 0.1 CH_4: 17.08
Ce-doped UIO-66-NH_2[3]	Visible light 20 mL H_2O 1 mL TEOA	CO: 9.99 CH_4:31.02
UIO-66-NH_2/$Ce(HCOO)_3$[4]	300 W Xe-lamp 20 mL H_2O 1 mL TEOA	CO: 40.18 CH_4:25.76
NH_2-UIO-66/TiO_2/Au[5]	150 W Ceramic-Metal-Halide Lamp Gas-Solid conditions	CO: 5.00 CH_4:27.2
NH_2-UIO-66/g-C_3N_4[6]	Visible light 20 mL H_2O 1 mL TEOA	CO: 4.33 CH_4:14.68

References

[1] X. Ma, T. Liu, J. Huang, J. Zhang, C. Yu and T. Huang. Journal of Environmental Chemical Engineering, 2026, 14, 122907

[2] J. Shi, X. Shi, L. Li, K. Lai, Y. Qiu, N. Li, Y. Gao and L. Ge. Chemical Engineering Journal, 2026, 538, 176961.

[3] Y. Xie, N. Yuan, H. Liu, L. Luo, J. Gong, X. Yin, T. Li and Y. Zhou. Applied Catalysis A: General, 2024, 674, 119616.

[4] N. Yuan, Y. Mei, Y. Liu, Y. Xie, B. Lin and Y. Zhou. Journal of CO_2 Utilization, 2022, 64, 102151.

[5] M. Duflot, C. Marchal, V. Caps, V. Artero, K. Christoforidis and V. Keller. Catalysis Today, 2023, 413-415, 114018.

[6] H. Liu, Y. Yang, C. Guo and Y. Zhou. Catalysis Science & Technology, 2024, 14, 5938-5948.